

## Analysis of MHD stability and active mode control on KSTAR for disruption prediction and avoidance

Y.S. Park<sup>1</sup>, S.A. Sabbagh<sup>1</sup>, B.H. Park<sup>2</sup>, J.H. Ahn<sup>1</sup>, J.W. Berkery<sup>1</sup>, H.S. Kim<sup>2</sup>, J.S. Kang<sup>2</sup>,  
 Y. Jiang<sup>1</sup>, J.M. Bialek<sup>1</sup>, J. Kim<sup>2</sup>, J.H. Lee<sup>2</sup>, M.J. Choi<sup>2</sup>, H.S. Han<sup>2</sup>, S.H. Hahn<sup>2</sup>, Y.M. Jeon<sup>2</sup>,  
 W.H. Ko<sup>2</sup>, J.S. Ko<sup>2</sup>, J.G. Kwak<sup>2</sup>, S.W. Yoon<sup>2</sup>, H.K. Park<sup>3</sup>, Z.R. Wang<sup>4</sup>, J.-K. Park<sup>4</sup>,  
 N.M. Ferraro<sup>4</sup>

<sup>1</sup> Department of Applied Physics, Columbia University, New York, NY, USA

<sup>2</sup> National Fusion Research Institute, Daejeon, Korea

<sup>3</sup> Ulsan National Institute of Science and Technology, Ulsan, Korea

<sup>4</sup> Princeton Plasma Physics Laboratory, Princeton, NJ, USA

Long-pulse plasma operation at high normalized beta,  $\beta_N$ , up to 4 (exceeding the  $n = 1$  ideal MHD no-wall stability limit) in KSTAR is presently limited by tearing instabilities [1] rather than resistive wall modes (RWMs). H-mode plasma operation during the 2018 KSTAR device campaign produced discharges having strong  $m/n = 2/1$  tearing instabilities at  $\beta_N \sim 1.6$  which is lower than the ideal MHD no-wall beta limit,  $\beta_N^{no-wall}$ , computed as 2.5 when the plasma internal inductance,  $l_i$ , is 0.7 for H-mode pressure profiles. Mode stability alteration was attempted by varying plasma heating, safety factor, collisionality, and rotation profile. The experiment confirmed that an extended duration of the electron cyclotron resonance heating (ECH) at the initial phase of the discharge plays a critical role in mode destabilization. The 105 GHz 2<sup>nd</sup> harmonic ECH with 630 kW power was injected to the plasma core region under an equilibrium toroidal magnetic field of 1.9 T with a total neutral beam heating power of 2.8 MW in the experiment. The ECH consistently produced an unstable tearing mode at the initial phase of discharge pulse ( $t_{onset} < 1.0$  s) in similar discharges having a long pulse duration up to 20 s. The initially insignificant magnitude of the mode increases due to a slow plasma current ( $I_p$ ) ramp up toward a flattop value of 650 kA with  $dI_p/dt = 53$  kA/s after the mode onset. The edge safety factor,  $q_{95}$ , decreased to 4.8 when the plasma reached the  $I_p$  flattop, and the mode amplitude measured by the external magnetic probes measuring poloidal field perturbations is sustained at a 25 G level for a long period of ~8 s (FIG. 1(a)) which is one of the highest rotating mode amplitude level measured in KSTAR to date. The mode starts to lock to the surrounding wall when its amplitude becomes greater than 25 G. By comparing the plasma to other discharges identically produced but without early ECH injection, it is confirmed that the highly unstable mode reduced  $\beta_N$  by ~20% and more significantly reduced toroidal plasma rotation by

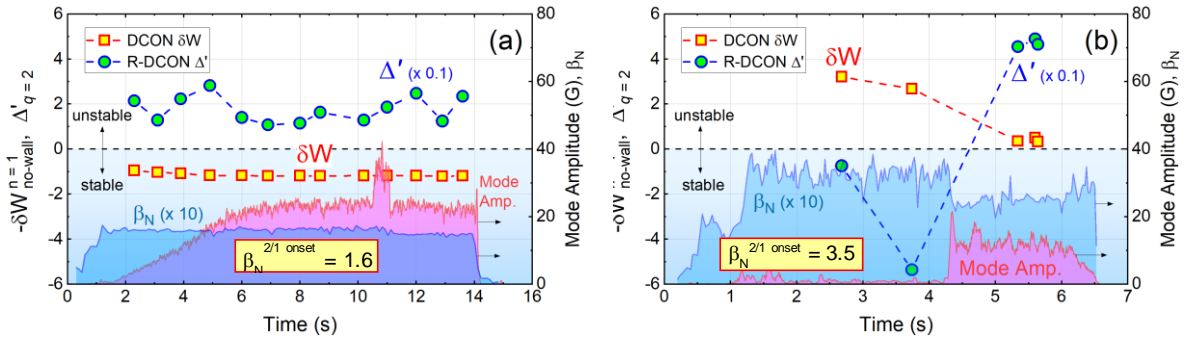


FIG. 1. The evolution of the  $n = 1$  no-wall stability criteria and the linear tearing stability index computed by DCON for the two discharges having 2/1 mode onset at (a) low  $\beta_N = 1.6$  and (b) higher  $\beta_N = 3.5$ , respectively. The measured mode amplitude and  $\beta_N$  are overlaid.

~50%. The 2D ECEI diagnostic confirmed that the electron temperature perturbation structure of the largely grown 2/1 mode exists across the estimated  $q = 2$  rational surface using the motional Stark effect (MSE) diagnostic data.

The ideal and resistive stability of the discharge discussed above is examined by using different physics models. The kinetic EFIT reconstructions that include constraints from Thomson scattering, charge exchange spectroscopy, MSE, and NUBEAM computed fast particle pressure are used as input to stability analysis for reliable calculation of stability which requires an accurate description of the pressure and  $q$ -profiles. The ideal  $n = 1$  stability, calculated by using the DCON code, is shown in FIG. 1(a). Negative total perturbed potential energy by  $n = 1$ ,  $\delta W_{no-wall}^{n=1}$ , indicates an unstable  $n = 1$  mode with no surrounding wall. The discharge equilibria show  $\delta W_{no-wall}^{n=1}$  consistently stays below the stability boundary and the  $n = 1$  ideal mode remains stable throughout the long discharge pulse. The stability of the observed 2/1 tearing mode is computed by using the resistive DCON code [2] and the M3D-C<sup>1</sup> code. The linear tearing stability index,  $\Delta'$ , at the  $q = 2$  surface computed by the resistive DCON shown in FIG. 1(a) indicates that there could be a destabilizing contribution from the linear tearing stability in the observed 2/1 mode at low  $\beta_N$  values. The effect of a finite island width which can generate somewhat reduced mode growth rate when an island enters in the non-linear regime is not considered in the present  $\Delta'$  analysis.

The stability result is compared to the mode that destabilized at significantly higher  $\beta_N \sim 3.5$  exceeding the computed  $\beta_N^{no-wall}$  shown in FIG. 1(b). The non-inductive current fraction ( $f_{NI}$ ) computed by TRANSP for these comparative discharges is also significantly different – 49% in the low  $\beta_N$  case (FIG. 1(a)) and 63% in the high  $\beta_N$  case (FIG. 1(b)). During the high  $\beta_N > 3$  phase with high  $f_{NI}$  before the 2/1 mode onset, the ideal mode is computed to be unstable while the RWM is experimentally stable in the discharge. The  $\beta_N^{no-wall}$  depends on  $l_i$  which is ~0.9 in the high  $\beta_N$  equilibria, and equilibria at high  $\beta_N/l_i$  ratio ~ 4 violate the ideal mode no-wall

stability criteria. The global MHD stability modified by kinetic effects can explain how RWMS at the achieved  $\beta_N > \beta_N^{no-wall}$  can remain stable [3]. At high  $\beta_N > 3$  in which 2/1 mode onset was observed in other discharges run with similar plasma conditions with a strong correlation between the mode onset and the coinciding ELM crash, a stable (negative)  $\Delta'$  is estimated and it changes to unstable values at reduced  $\beta_N$  later in the discharge similarly to the low  $\beta_N$  case in FIG. 1(a). The result is consistent with the neoclassical tearing modes (NTMs) generally being linearly stable in the previous studies [4]. At  $\beta_N$  above the ideal stability boundary, the computed  $\Delta'$  is found to be more sensitive to the reconstructed current profile than in the case of lower  $\beta_N$ . The linear stability calculation using the M3D-C<sup>1</sup> code shows an unstable global mode for the high  $\beta_N$  equilibria consistent with the DCON analysis. Tearing modes are computed to be mostly stable which suggests that the unstable linear  $\Delta'$  computed for the equilibria at the saturated mode phase may not exactly represent the stability. The plasma resistivity estimated by TRANSP using the Spitzer formula is used as input in the M3D-C<sup>1</sup> calculations, and the resistive wall model used in the analysis enables more reliable stability analysis by including the response of the conducting wall.

The destabilizing effect of the bootstrap current ( $J_{BS}$ ) in the NTM stability,  $\Delta'_{NC}$ , is computed by TRANSP which is given by  $\Delta'_{NC}(w) = k_{NC} 16 J_{BS} / (s w \langle J \rangle)$  [5]. Here  $w$  is the island width,  $s$  is the magnetic shear,  $\langle J \rangle$  is the average current density for the inner region from the mode rational surface  $0 < r < r_s$ , and  $k_{NC}$  is a calibration coefficient. The magnitude of the destabilization effect,  $|\Delta'_{NC}| = 16 J_{BS} / (s \langle J \rangle)$ , is computed to be large with values in the range 2.4–2.8 for the high  $\beta_N > 3$  equilibria in FIG. 1(b) in which the NTM stability is expected to be unstable. The  $|\Delta'_{NC}|$  becomes significantly lower ranging from 0.6 to 0.9 after the island saturates and the confinement is consequently degraded.

In preparation for long-pulse plasma operation at higher beta utilizing increased plasma heating power in 2019, a RWM active feedback control algorithm has been completed and enabled on KSTAR. An algorithm has been developed that includes sensor compensation of the induced current on the passive conductors (AC compensation) by following an approach similar to that used in NSTX. In KSTAR, the feedback coils are at the midplane whereas the mode measurement is made off-midplane, hence the effect of varied mode helicities on the optimal feedback phase can be mitigated when the mode phase measured above and below the midplane are combined. Use of multiple sensor arrays is enabled by modifying the sensor toroidal angles assumed in mode decomposition. This gives the effect of toroidally rotating the sensor arrays with respect to each other. To determine the proper amount of angle shift, the

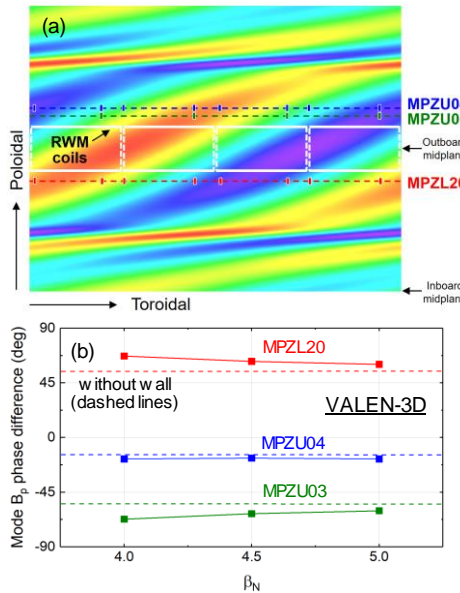


FIG. 2. (a) The perturbed poloidal magnetic field for the unstable  $n = 1$  eigenfunction with no wall. (b) The mode phase measured by the sensor arrays with respect to the phase at the midplane.

poloidal field perturbation by a simulated unstable RWM is analyzed with varied mode growth rate represented by varying  $\beta_N$ . Figure 2(a) shows the poloidal field perturbation from a projected unstable RWM with the positions of the RWM sensors and coils overlaid. Although the sensor arrays are positioned closely to each other at the region where the phase of the perturbed mode field does not significantly change along the poloidal direction, the mode phase measured by these arrays in 3D space computed by the VALEN-3D code can be significantly different. In FIG. 2(b), the change in the toroidal phase of the measured mode field with respect to the phase measured at the outboard midplane is shown.

The phase difference between the midplane and off-

midplane region changes by up to  $7^\circ$  with the  $\beta_N$  values examined as the mode eigenfunction shape changes at higher  $\beta_N$ . The mode decomposition matrix which computes the amplitude and the toroidal phase of the RWM is generated by considering these sensor phase shifts. The developed mode identification and feedback algorithm has been implemented in the real-time plasma control system in KSTAR. This analysis on stability, transport, and active mode control provides the required foundation for disruption prediction and avoidance research on KSTAR. This work is supported by US DOE Grant DE-SC0016614.

## References

- [1] Y.S. Park, S.A. Sabbagh, W.H. Ko, *et al.*, “Investigation of instabilities and rotation alteration in high beta KSTAR plasmas”, *Phys. Plasmas* **24** (2017) 012512.
- [2] A.H. Glasser, Z.R. Wang, J.-K. Park, “Computation of resistive instabilities by matched asymptotic expansions”, *Phys. Plasmas* **23** (2016) 112506.
- [3] J.W. Berkery, S.A. Sabbagh, R. Betti, *et al.*, “Resistive wall mode instability at intermediate plasma rotation”, *Phys. Rev. Lett.* **104** (2010) 035003.
- [4] R.J. La Haye, “Neoclassical tearing modes and their control”, *Phys. Plasmas* **13** (2006) 055501.
- [5] E.D. Fredrickson, “Observation of spontaneous neoclassical tearing modes”, *Phys. Plasmas* **9** (2002) 548.